

# The Nucleotide-Dependent Interactome of Rice Heterotrimeric G-Protein $\alpha$ -Subunit

Akshaya Kumar Biswal, Evan Wesley McConnell, Emily Grace Werth, Shuen-Fang Lo, Su-May Yu, Leslie M. Hicks, and Alan M. Jones\*

**The rice heterotrimeric G-protein complex, a guanine-nucleotide-dependent on-off switch, mediates vital cellular processes and responses to biotic and abiotic stress. Exchange of bound GDP (resting state) for GTP (active state) is spontaneous in plants including rice and thus there is no need for promoting guanine nucleotide exchange in vivo as a mechanism for regulating the active state of signaling as it is well known for animal G signaling. As such, a master regulator controlling the G-protein activation state is unknown in plants. Therefore, an ab initio approach is taken to discover candidate regulators. The rice  $G\alpha$  subunit (RGA1) is used as bait to screen for nucleotide-dependent protein partners. A total of 264 proteins are identified by tandem mass spectrometry of which 32 were specific to the GDP-bound inactive state and 22 specific to the transition state. Approximately, 10% are validated as previously identified G-protein interactors.**

Rice G-proteins constitute a membrane-tethered complex that controls fundamental processes involving environmental cues that impact development and stress responses.<sup>[1–3]</sup> Our understanding of the composition of the rice G-protein complex is limited but more importantly, we do not know what component(s) regulate the active state of the complex. The canonical rice heterotrimeric G-protein complex comprises a guanine-nucleotide-binding  $G\alpha$  subunit (RGA1) and an obligate  $G\beta\gamma$  dimer (RGB1 and one of 5  $G\gamma$  subunits).<sup>[1,4]</sup> In

addition to the canonical  $G\alpha$  subunit, rice encodes three atypical extra-large  $G\alpha$  (XLG) subunits,<sup>[5]</sup> although those are not yet shown to be a physical part of the rice complex as was shown for the Arabidopsis G-protein complex. The G-protein complex is inactive when  $G\alpha$  is bound to GDP while the GTP-bound complex is active.<sup>[6,7]</sup> Deactivation occurs through hydrolysis of the bound GTP to form GDP by the intrinsic GTPase activity of the  $G\alpha$  subunit. This step cycles through a short-lived transition state – GDP+Pi. The activated  $G\alpha$  separates from the  $G\beta\gamma$  dimer and consequently both target their corresponding effectors to amplify the active state. In animals, 7-transmembrane (7-TM) cell surface G-protein-coupled rec-

eptors (GPCRs) catalyze the GDP/GTP nucleotide exchange, but nucleotide exchange is spontaneous in plant cells<sup>[8]</sup> and therefore plants do not utilize 7-TM GPCRs.<sup>[9]</sup> Rather, in most plants, a 7-TM Regulator of G Signaling (RGS) protein modulates the G-protein activation state by ligand-dependent de-repression.<sup>[7,10]</sup> The prototype for this hybrid GPCR-GTPase accelerating protein (GAP) architecture is Arabidopsis RGS1 (AtRGS1).<sup>[7]</sup> AtRGS1 accelerates the intrinsic GTPase activity of the Arabidopsis  $G\alpha$  subunit (AtGPA1) to promote the inactive (OFF) state by stabilizing the transition state,<sup>[11]</sup> consequently facilitating re-binding with the  $\beta\gamma$  dimer to form the heterotrimeric complex and to maintain the G-protein complex in the inactive state.<sup>[12]</sup> In addition, AtRGS1 binds tyrosine phosphorylated AtGPA1 in its GDP-bound state by an unprecedented mechanism dubbed “substrate phosphoswitching”<sup>[13]</sup> Ligand-dependent endocytosis of AtRGS1 protein physically uncouples itself and its GAP activity from the  $G\alpha$  protein, consequently de-repressing the G cycle to allow self-activation.<sup>[10]</sup> All tested eudicots and monocots except some cereals have 7TM-RGS molecules, which interact with their cognate  $G\alpha$  subunits and maintain those in their resting state.<sup>[14]</sup> Rice is among those cereals that does not have a 7TM-RGS protein.<sup>[15]</sup>

The 7-transmembrane RGS is not likely the master regulator of the G-protein activation state in plants because genetic ablation of the prototype 7TM RGS protein (AtRGS1) does not confer the full phenotype that is generated by the loss of the entire G-protein complex.<sup>[7,16–18]</sup> Additionally cereals typically lack 7TM RGS.<sup>[10,19]</sup> Therefore, rice represents an excellent model to uncover a novel mechanism of G-protein regulation that functions in rice and

Dr. A. K. Biswal, Dr. A. M. Jones  
Department of Biology  
University of North Carolina at Chapel Hill  
Chapel Hill, NC 27599, USA  
E-mail: alan\_jones@unc.edu

Dr. McConnell, Dr. E. G. Werth, Prof. L. Hicks  
Department of Chemistry  
University of North Carolina at Chapel Hill  
Chapel Hill, NC 27599, USA

Dr. S. F. Lo, Prof. S. M. Yu  
Institute of Molecular Biology  
Academia Sinica, Nankang  
Taipei, Taiwan, China

Dr. A. M. Jones  
Department of Pharmacology  
University of North Carolina at Chapel Hill  
Chapel Hill, NC 27599, USA

 The ORCID identification number(s) for the author(s) of this article can be found under <https://doi.org/10.1002/pmhc.201800385>

DOI: 10.1002/pmhc.201800385

related cereals and thus an ab initio search for the master regulator in rice is a valid approach. Such an approach could incorporate a screen for proteins that interact with RGA1 in a nucleotide-dependent manner. There are three characterized nucleotide-bound isoforms of  $G\alpha$  subunits: GDP-bound, GTP-bound, and the transition state of GDP+Pi bound. Structural studies indicate that the  $G\alpha$  complexed with GDP ( $G\alpha\cdot\text{GDP}$ ) represents the deactivated/inactive form of  $G\alpha$ .<sup>[20–22]</sup> GTP-binding causes a charge and steric-induced conformational change leading to dissociation of the  $G\beta\gamma$  dimer. Consequently, exposure of this protein-protein interface makes accessible interaction with target proteins called effectors that become activated in turn. Known regulators do not interact with this state. Rather, modulators of G cycling recognize the transition state.<sup>[23]</sup> This GDP+Pi transition state can be mimicked using GDP plus fluoride complexes of aluminum ( $\text{AlF}_4^-$ ) that act as analogues of the  $\gamma$ -phosphate of GTP in the nucleotide site of  $G\alpha$  bound to  $G\alpha\cdot\text{GDP}$ .<sup>[24]</sup> In addition, NMR studies show that  $\text{Mg}^{2+}\cdot\text{GDP}\cdot\text{AlF}_4$  mimics  $\text{Mg}^{2+}\cdot\text{GTP}$  in its capacity to activate the G-protein  $\alpha$  subunit.<sup>[25]</sup> For this study, we assume that regulators of RGA1 interact either with the  $G\alpha\cdot\text{GDP}$  or  $G\alpha\cdot\text{GDP}\cdot\text{AlF}_4^-$  complex and that non-regulatory effectors interact with the GTP-bound state.

The experimental scheme for nucleotide-dependent interactors of RGA1 is shown in **Figure 1** and all other details regarding methods used in this study are provided in Supporting Information. A homology model of RGA1 was constructed

by the Modeller software using *Arabidopsis thaliana*  $G\alpha$  subunit, chain A (AtGPA1, PDB = 2XTZ)<sup>[26]</sup> as the template (Figure S1, Supporting Information). All four loop regions were further refined and the best model with the lowest DOPE score for the whole molecule was selected. The DOPE score for individual residues plotted against the corresponding template residue showed a close similarity in their energy levels (Figure S2, Supporting Information). Two antigenic epitopes, located sterically opposite to each other, were chosen for development of antibodies. Epitope A was located at the C-terminus while epitope B was located around the switch II region (Figure S1, Supporting Information). As shown in Fig. 1A, two polyclonal antibodies were developed for this screen targeting both epitopes. Both antibodies showed high avidity to the recombinant RGA1 (Figure S3, Supporting Information). All antisera cross react to non-antigen proteins at some titer and/or detection level. When blots are over developed, it can be observed that Antibody A weakly recognizes some proteins in the crude protein extracted from DK22 plantlets (Figure S3A, Supporting Information). At low dilution, antibody B can recognize two other bands (Figure S3B, Supporting Information). This highlights the importance of using multiple antibodies and including negative controls in a tandem MS approach. Both antibodies were independently immobilized to the resin to display recombinant RGA1 in the presence of buffer containing  $\text{Mg}^{2+}\cdot\text{GDP}$  or  $\text{Mg}^{2+}\cdot\text{GDP}\cdot\text{AlF}_4^-$ . The immobilized recombinant RGA1 served as the bait for its interactors in the tissue extracts of DK22 (*rga1* mutant in the landrace Nipponbare). The Sypro-Ruby staining pattern of the bands of immunoprecipitation eluates was clearly different for each pull-down, which indicated that different number of proteins were pulled for inactive and transition phase states than the control pull down without RGA1 (Figure S4, Supporting Information). Three biological replicates were obtained with each resin-linked antibody to reduce false positives. Protein identification was performed using Mascot (Matrix Science, London, UK; v2.5.1) against the *Oryza sativa* subsp. japonica UniProtKB database (Proteome ID: UP000059680) after the sequences for common laboratory contaminants were removed (<http://www.thegpm.org/cRAP/>, 116 entries). High-confidence interactors were identified by analyzing the affinity-purification mass spectrometry experiments data using Progenesis Q1 and then filtering through SAINT analysis as described in the Supporting Information. Finally, only those interactors were considered which showed at least 2-fold mean abundance than the negative control. This screening identified a total of 264 candidate RGA1-interacting proteins using two different antibodies that targeted either of two antigenic regions located at the opposite sides of the RGA1 3D-model to generate two presentations for interactor capture (Figure S1, Supporting Information). There were 210 interactors identified for antibody A capture and 140 for antibody B capture (Table S1, Supporting Information). Among these, 85 proteins were shared between both presentation conformations, while the rest were unique to either A or B (Table S1, Supporting Information). A high number of candidate RGA1 interactors is expected given that the rice heterotrimeric G-protein forms a large 400-kDa complex.<sup>[27,28]</sup> It is unknown if the nucleotide-binding state of proteins affect the antigen-antibody interaction, however, if this did occur, binding was not rate limiting because we observed that the

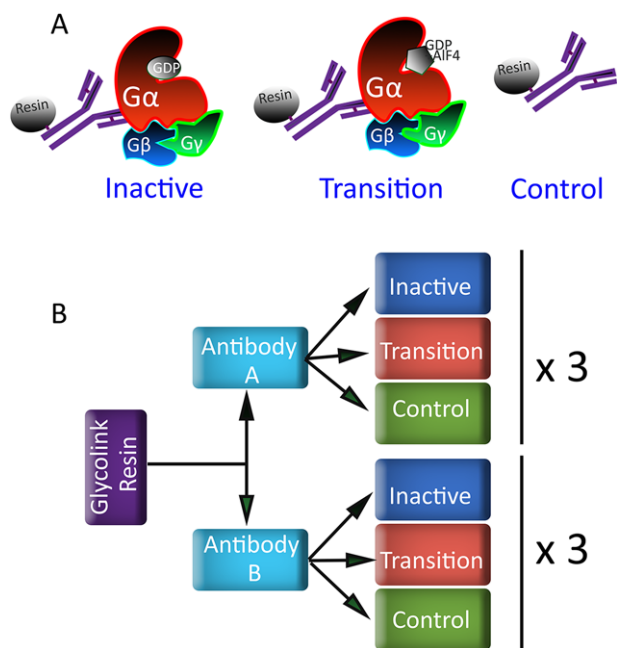


**Figure 1.** Experimental design of the immunoprecipitation assay and sample replication. A) RGA1 was presented as a bait to protein extracts of DK22 plantlets in its inactive state (GDP bound, +GDP) or in its transition state (GDP+Pi, +AlF<sub>4</sub>). As a negative control, these protein extracts were run on a column with immobilized antibody lacking RGA1. B) Two different antibodies (A<sub>4</sub> and B<sub>4</sub>) were used to present RGA1 to interacting proteins in the rice extract. The experiment was performed with three independent biological replicates (3×) for both antibodies plus the three negative controls for each antibody.

**Table 1.** List of nucleotide-dependent RGA1 interactors. Thirty two interactors showed nucleotide specificity for the GDP-bound inactive form of RGA1 while 22 of them showed specificity for the GDP+Pi bound transition state of RGA1.

Inactive (GDP-bound)		Transition (GDP+Pi or ALF4- bound)	
UniprotId	Description	UniprotId	Description
Q7XS58	Cysteine synthase [1.12]	Q5ZBX1	40S ribosomal protein S4 [1.08]
Q10NY2	Protein TPR3 [1.06]	Q6K3Z3*	Os09g0252100 protein [1.36]
Q2QLY4	5-methyl tetrahydropteroyl triglutamate [1.19]	Q8LQ70	Os01g0742300 protein [1.14]
<b>Q75193</b>	Beta-glucosidase 7 [1.18]	Q6YYR2	Os08g0234000 protein [1.11]
Q84TA3	Leukotriene A-4 hydrolase homolog [1.04]	Q5JN29	Os01g0959900 protein [1.64]
<b>B7EIQ8</b>	Os02g0125700 protein [1.10]	<b>Q2R011</b>	Dirigent protein [1.49]
Q5W730	Os05g0333500 protein [1.13]	Q0JA12	OSJNba0093F12.16 protein [1.30]
Q8S718	Glutathione S-transferase GSTU6 [1.12]	<b>Q7XSQ9</b>	Probable aquaporin PIP1-2 [1.23]
Q75G13	Tubulin alpha chain [1.09]	Q6Z2T6	Geranylgeranyl diphosphate reductase, chloroplastic [1.03]
<b>Q6L451</b>	ATP-dependent Clp protease proteolytic sub [1.25]	<b>Q6ATY4</b>	UPF0603 protein Os05g0401100, chloroplastic [1.27]
Q6ER90	Os02g0538000 protein [1.24]	Q10MJ1	Probable glutamyl endopeptidase, chloroplastic [1.33]
Q656T5	Os01g0574600 protein [1.40]	P0C470	30S ribosomal protein S15, chloroplastic [1.37]
A0A0P0WP33	Phosphoglycerate kinase [1.08]	<b>P0C355</b>	Photosystem I P700 chlorophyll a apoprotein A1 [1.14]
<b>A0A0N7KNM4</b>	Os07g0548300 protein [1.21]	<b>Q9L677</b>	Os01g0191200 protein [1.45]
Q8S6N5	Acetyl-CoA carboxylase [1.11]	<b>Q75HW4</b>	Os05g0395000 protein [2.86]
Q7XPL2	Oxygen-dependent coproporphyrinogen-III oxidase [1.31]	Q0D3Q1	Os07g0673500 protein [1.06, 3.85]
Q6Z9A3	Probable mannose-1-phosphate guanylyltransferase 3 [1.29]	Q2QTC2	Phosphoglucan, water dikinase, chloroplastic [1.12]
Q5VRY1	18.0 kDa class II heat shock protein [1.37]	Q0DG31	Os05g0556100 protein [1.89]
P93431	Ribulose biphosphate carboxylase/oxygenase activase, chloroplastic [1.13]	Q654U5	Os06g0247800 protein [1.96]
Q851Y6	Os03g0851300 protein [1.21]	Q84LG6	Eukaryotic translation initiation factor 3 subunit C [2.5]
Q6K3Z3*	Os09g0252100 protein [1.36]	Q6YYB9	Tryptophan synthase [1.02]
Q7F911	Chaperone protein ClpC1, chloroplastic [1.10]	Q6ZDR7	Os08g0486200 protein [2.99]
Q10A14	Alanine-tRNA ligase [1.40]		
Q2QSR7	Os12g0420200 protein [1.29]		
Q5VME5	Glycosyltransferase [1.21]		
Q8GVZ0	Os07g0546000 protein [1.69]		
Q2QX45	Calcium-dependent protein kinase 28 [1.33]		
Q6L506	Probable monofunctional riboflavin biosynthesis protein RIBA 3, chloroplastic [1.14]		
Q5JLP6	S-formylglutathione hydrolase [1.33]		
Q5QMH1	RuvB-like helicase [1.47]		
Q7F270	ADP-ribosylation factor 1 [1.63]		
<b>Q84M73</b>	Expressed protein [7.66]		

\*indicates that this protein changes its nucleotide specificity when presented with different antibodies. Bold indicates that these proteins were predicted to have transmembrane domains. The numbers in brackets are the fold change ratio between both nucleotide specific states.

recombinant RGA1 was the highest abundant protein in the pool in all cases for both antibodies and for both nucleotide-binding stages, verifying that the antibodies, bind to RGA1 in both nucleotide-binding states. The interactors were classified based upon their nucleotide dependence i.e. preference to the inactive and transition state of RGA1. Proteins with peptide count ratio of control to inactive < 0.5 but control to transition phase > 0.5 were labeled as inactive phase specific. Similarly, proteins with peptide count ratio of control to transition < 0.5 but control to inactive phase > 0.5 were labeled as transition phase specific, respectively. As listed in **Table 1**, 32 and 22 proteins, respectively, were specific to the inactive state and transition stage of RGA1 based on the above criterion (Table S1, Supporting Information). One of the

hypothetical proteins (Q84M73), which was also predicted as a membrane protein in our analysis, showed more than a 7-fold specificity towards the inactive stage of RGA1, which indicates that either this protein plays a role in stabilizing the inactive stage<sup>[29]</sup> or regulates the cycling by binding to the inactive state. A putative acetyl-CoA C-acyltransferase (Q6K3Z3) showed preference to the transition phase of RGA1 when presented with antibody A but its preference changed to inactive phase when presented with antibody B. Expression of an ortholog of this protein was reported to be associated with internode elongation in bamboo.<sup>[30]</sup> It should be noted that d1 (Gα) null mutants have short internodes. This intriguing observation may be due to a change in conformation of the RGA1 due to

antibody binding. We assumed that a regulator of the activation state of the G-protein would perceive extracellular signals and therefore would be an integral membrane protein. Therefore, we analyzed the candidate regulators for transmembrane topology, in particular 7TM topology in analogy to AtRGS1 and GPCR architecture. All proteins were analyzed by TMHMM 2.0, SOSUI and dense alignment surface (DAS) servers. Thirty proteins were identified to have one or more transmembrane domains by at least two of the above programs (Table S1, Supporting Information, membrane protein sheet).

Orthologs of 22 candidate interactors identified here were reported to interact with rice or Arabidopsis G-proteins subunits (Table S1, Supporting Information, interactors sheet, column P, Orthologous interactions previously reported, references). For example, orthologs to eight AGB1 interactors were found in our interactome that are involved in protein folding, calcium ion binding, cellular macromolecule biosynthetic process and calcium-dependent phospholipid binding process.<sup>[31]</sup> Seven orthologous AtRGS1 interactors<sup>[32]</sup> are involved in DNA binding, GTP-binding, photosynthesis, cellulose and L-ascorbic acid biosynthetic process and five orthologs<sup>[33]</sup> are involved in ubiquinol-cytochrome-c reductase activity and L-phenylalanine biosynthesis.

Phosphorylation plays an important role in regulating the G-protein activation state.<sup>[13]</sup> We observed five cytosolic kinases/dikinases as well as two serine/threonine-protein phosphatase in our interactome (Table S1, Supporting Information). Calcium-dependent protein kinase 28, (Q2QX45), which has high structural similarity with SnRK2 kinase, preferentially binds to the inactive state of RGA1. Both AtGPA1 and SnRK2 are involved in abscisic acid (ABA) signaling.<sup>[34,35]</sup> Therefore, OsCPK28 may function in conjunction with RGA1 in the ABA signaling pathway. Protein phosphatases also regulate ABA signaling.<sup>[36]</sup> Serine/threonine protein phosphatases drive exocytosis in major secretory systems.<sup>[37]</sup> Both of these phosphatases are cytosolic and may be involved in regulating the phosphorylation state of RGA1. The highest fraction (56.06%) of the interactors were annotated as “catalytic activity”, about 23% were annotated for different “binding activities”, and 0.5% were annotated as “signal transduction activity”. The rest of the interactors were annotated as structural molecule activity, transporter activity, receptor activity and translation regulator activity (Table S1, Supporting Information). The highest portion (42.5%) of the interactors were annotated as metabolic processes followed by 33.5% annotated in different cellular processes. In relation to the biological process, the highest fraction (44%) of proteins were related to various metabolic processes followed by cellular process. Several proteins (4.3% of this interactome) are categorized as “response to stimulus” and  $\approx 1/3$  of these (1.6%) were subdivided into “biological regulation”. Approximately 1% of the proteins were associated with various developmental process in which G-proteins are known to play an indirect role. A considerable fraction (8%) of the RGA1 interactors were either membrane localized or present in the cell junction consistent with our prediction of 30 membrane proteins within this interactome. Ninety-eight interactors were located either in organelles or macromolecular complexes. A large fraction (18.5%) of interactors were classified as nucleic acid-binding proteins consistent with our previous finding of transcription factors within the Arabidopsis

G protein interactome<sup>[33]</sup>. Hydrolases and oxidoreductases covered 16.5 and 12.5% of the interactors, respectively. A. thaliana Nudix hydrolase AtNUDT7 plays important role in cellular response to diverse biotic and abiotic stresses by forming complexes with RACK1A protein and G $\gamma$  subunits of the signal transducing heterotrimeric G-protein.<sup>[38]</sup> Certain oxidoreductase proteins are located at the membrane/cytoskeleton area where they act as adaptors to receive signals from the cell surface.<sup>[39]</sup> Numerous hypotheses were proposed for the role of redox enzymes within the plasma membrane such as regulation of cell signaling, cell growth, apoptosis, proton pumping, and ion channels.<sup>[40]</sup> For example, acireductone dioxygenase is a known redox enzyme involved in the G-protein pathway.<sup>[41]</sup>

In summary, we identified 264 potential interactors of RGA1, which includes several membrane proteins and proteins that preferentially interact with the nucleotide-bound state of RGA1.

## Supporting Information

Supporting Information is available from the Wiley Online Library or from the author.

## Acknowledgements

The authors thank Ben Webb and Brenda Temple for helpful comments developing the structural model of RGA1. This work was supported by a USDA NIFA Agriculture and Food Research grant to A.M.J. (2015-06576). Protein interactions are deposited to BioGRID <https://thebiogrid.org/uponjournalacceptance>.

## Conflict of Interest

The authors declare no conflict of interest.

## Keywords

rice, heterotrimeric G protein, tandem mass spectrometry

Received: November 5, 2018

Revised: February 12, 2019

Published online: April 18, 2019

- [1] D. Urano, J.-G. Chen, J. R. Botella, A. M. Jones, *Open Biol.* **2013**, *3*, 120186.
- [2] A. M. Jones, S. M. Assmann, *EMBO Rep.* **2004**, *5*, 572.
- [3] J. R. Botella, *Trends Plant Sci.* **2012**, *17*, 563.
- [4] M. G. Mason, J. R. Botella, *Proc. Natl. Acad. Sci. U. S. A.* **2000**, *97*, 14784.
- [5] Y. Iwasaki, H. Kato, Y. Fujisawa, K. Oki, *Biotechnol. Agric. For.* **2008**, *1*, 135–148.
- [6] K. Oki, Y. Fujisawa, H. Kato, Y. Iwasaki, *Plant Cell Physiol.* **2005**, *46*, 381.
- [7] J.-G. Chen, F. S. Willard, J. Huang, J. Liang, S. A. Chasse, A. M. Jones, D. P. Siderovski, *Science* **2003**, *301*, 1728.
- [8] D. Urano, J. C. Jones, H. Wang, M. Matthews, W. Bradford, J. L. Benetzen, A. M. Jones, *PLoS Genet.* **2012**, *8*, e1002756.

- [9] D. Urano, A. M. Jones, *Plant Physiol.* **2013**, *161*, 1097.
- [10] D. Urano, N. G. Phan, J. C. Jones, J. Yang, J. Huang, J. Grigston, J. P. Taylor, A. M. Jones, *Nat. Cell Biol.* **2012**, *14*, 1079.
- [11] D. M. Berman, T. Kozasa, A. G. Gilman, *J. Biol. Chem.* **1996**, *271*, 27209.
- [12] J. C. Jones, B. R. S. Temple, A. M. Jones, H. G. Dohlman, *J. Biol. Chem.* **2011**, *286*, 13143.
- [13] B. Li, M. Tunc-Ozdemir, D. Urano, H. Jia, E. G. Werth, D. D. Mowrey, L. M. Hicks, N. V. Dokholyan, M. P. Torres, A. M. Jones, *J. Biol. Chem.* **2018**, *293*, jbc.RA117.000163.
- [14] N. G. Phan, D. Urano, M. Srba, L. Fischer, A. M. Jones, *Plant Signal Behav.* **2012**, *8*, 8.
- [15] D. Urano, T. Dong, J. L. Bennetzen, A. M. Jones, *Mol. Biol. Evol.* **2015**, *32*, 998.
- [16] J.-P. Huang, M. Tunc-Ozdemir, Y. Chang, A. M. Jones, *Front. Plant Sci.* **2015**, *6*, 851.
- [17] D. Urano, K. Miura, Q. Wu, Y. Iwasaki, D. P. Jackson, A. M. Jones, *Plant Cell Physiol.* **2016**, *57*, 437.
- [18] Y. Chen, F. Ji, H. Xie, J. Liang, J. Zhang, *Plant Physiol.* **2006**, *140*, 302.
- [19] D. Hackenberg, M. R. McKain, S. G. Lee, S. Roy Choudhury, T. McCann, S. Schreier, A. Harkess, J. C. Pires, G. K.-S. Wong, J. M. Jez, E. A. Kellogg, S. Pandey, *New Phytol.* **2016**.
- [20] J. Sondek, D. G. Lambright, J. P. Noel, H. E. Hamm, P. B. Sigler, *Nature* **1994**, *372*, 276.
- [21] M. Simon, M. Strathmann, N. Gautam, *Science* **1991**, *252*, 802.
- [22] J. J. Tesmer, D. M. Berman, A. G. Gilman, S. R. Sprang, *Cell* **1997**, *89*, 251.
- [23] S. R. Sprang, *Biopolymers* **2016**, *105*, 449.
- [24] J. Bigay, P. Deterre, C. Pfister, M. Chabre, *EMBO J.* **1987**, *6*, 2907.
- [25] T. Higashijima, M. P. Grazianosli, H. Sugall, M. Kainosho, A. G. Gilman, *J. Biol. Chem.* **1991**, *266*, 3396.
- [26] J. C. Jones, J. W. Duffy, M. Machius, B. R. S. Temple, H. G. Dohlman, A. M. Jones, *Sci. Signal.* **2011**, *4*, ra8.
- [27] S. Li, W. Liu, X. Zhang, Y. Liu, N. Li, Y. Li, *Plant Signal. Behav.* **2012**, *7*, 1357.
- [28] C. Kato, T. Mizutani, H. Tamaki, H. Kumagai, T. Kamiya, A. Hirobe, Y. Fujisawa, H. Kato, Y. Iwasaki, *Plant J.* **2004**, *38*, 320.
- [29] D. P. Siderovski, F. S. Willard, *Int. J. Biol. Sci.* **2005**, *1*, 51.
- [30] K. Cui, C. Y. He, J. G. Zhang, A. G. Duan, Y. F. Zeng, *J. Proteome Res.* **2012**, *11*, 2492.
- [31] Y. Yu, D. Chakravorty, S. M. Assmann, *Plant Physiol.* **2018**, *176*, 2426.
- [32] D. K. Jaiswal, E. G. Werth, E. W. McConnell, L. M. Hicks, A. M. Jones, *Curr. Plant Biol.* **2016**, *5*, 25.
- [33] K. Klopffleisch, N. G. Phan, K. Augustin, R. S. Bayne *Mol. Syst. Biol.* **2011**, *7*, 1.
- [34] L.-M. Ng, F.-F. Soon, X. E. Zhou, G. M. West, A. Kovach, K. M. Suino-Powell, M. J. Chalmers, J. Li, E.-L. Yong, J.-K. Zhu, P. R. Griffin, K. Melcher, H. E. Xu, *Proc. Natl. Acad. Sci.* **2011**, *108*, 21259.
- [35] X. Q. Wang, H. Ullah, A. M. Jones, S. M. Assmann, *Science* **2001**, *292*, 2070.
- [36] K. Wang, J. He, Y. Zhao, T. Wu, X. Zhou, Y. Ding, L. Kong, X. Wang, Y. Wang, J. Li, C.-P. Song, B.-S. Wang, S. Yang, J.-K. Zhu, Z. Gong, *Plant Cell* **2018**, *30*, 815.
- [37] A. T. R. Sim, M. L. Baldwin, J. A. P. Rostas, J. Holst, R. I. Ludowyke, *Biochem. J.* **2003**, *373*, 641.
- [38] K. Olejnik, M. Bucholc, A. Anielska-Mazur, A. Lipko, M. Kujawa, M. Modzelan, A. Augustyn, E. Kraszewska, *Acta Biochim. Pol.* **2011**, *58*, 609.
- [39] J. Y. Chang, R. Y. He, H. P. Lin, L. J. Hsu, F. J. Lai, Q. Hong, S. J. Chen, N. S. Chang, *Exp. Biol. Med.* **2010**, *235*, 796.
- [40] M. A. Baker, A. Lawen, *Antioxid. Redox Signal.* **2000**, *2*, 197.
- [41] E. J. Friedman, H. X. Wang, K. Jiang, I. Perovic, A. Deshpande, T. C. Pochapsky, B. R. S. Temple, S. N. Hicks, T. K. Harden, A. M. Jones, *J. Biol. Chem.* **2011**, *286*, 30107.